From MonoBINOL to BisBINOL: Expanded Enantioselective Fluorescent Recognition of Amino Acids

Bingyi Huo,[a], Kai Lu,[a] Jun Tian,[a] Feng Zhao,[a] Yalin Wang,[a] Shanshan Yu,*[a] Xiaoqi Yu,[a] Lin Pu*[b]

[a]Key Laboratory of Green Chemistry and Technology, Ministry of Education, College of Chemistry, Sichuan University, Chengdu, China 610064
[b]Department of Chemistry, University of Virginia, McCormick Rd, Charlottesville VA 22904.
E-mail: lp6n@virginia.edu yushanshan@scu.edu.cn

Abstract. Condensation of (*R*)-3,3'-diformyl-1,1'-bi-2-naphthol (BINOL) with (pyridine-2,6-diylbis(methylene))bis(triphenyl phosphonium) dibromide in the presence of a base gave a new bisBINOL-based fluorescent probe (*R,R*)-**4**. This compound shows expanded substrate scope in the recognition of amino acids with good enantioselective fluorescent responses toward 17 naturally occurring common amino acids. Two diastereomeric imines were synthesized from the condensation of (*R,R*)-**4** with *L*- and *D*-valine and the reactions of these imines with $Zn(OAc)_2$ were investigated by various spectroscopic methods for better understanding on the enantioselective fluorescent recognition process.

Introduction

Because of the importance of chiral amino acids in biology and synthesis, significant research has been conducted in the development of fluorescent probes to discriminate the enantiomers of amino acids in recent years.[1-5] In comparison with other analytical methods, the fluorescence-based detection has the advantages of easily available equipment, high sensitivity, real time imaging and online monitoring. In 2014, we reported that the 1,1'-bi-2-naphthol (BINOL)-based compound (*S*)- or (*R*)-**1** in combination with Zn^{2+} showed enantioselective fluorescent response toward certain amino acids.[6] In order to further improve this fluorescent probe in chiral analysis, we have undertaken several strategies to modify its structure. We found that condensation of (*R*)-**1** with a diWittig's reagent can readily generate a bisBINOL compound which has shown significantly enhanced enantioselectivity and greatly expanded substrate scope in the fluorescent recognition of amino acids. Herein, these results are reported.

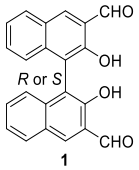

1

Results and Discussion

1. Design and Synthesis of a BisBINOL-Pyridine-Based Molecular Probe

Scheme 1 shows our synthesis of the bisBINOL compound (*R,R*)-**4**, newly designed for the recognition of amino acids. Reaction of the MOM-protected BINOL aldehyde (*R*)-**2**[7] with (pyridine-2,6-diylbis(methylene))bis(triphenyl phosphonium) dibromide[8] in the presence of t-BuOK at 0 °C gave compound (*R,R*)-**3** in 43% yieldThe MOM protecting groups of (*R,R*)-**3** were removed with HCl (conc.) to give the desired product (*R,R*)-**4** in 91% yield. The ^{1}H NMR spectrum of (*R,R*)-**4** in DMSO-d_6 gave a signal at δ 10.18 for the two hydroxyl protons *ortho* to the aldehyde groups on the naphthalene rings similar to that observed in **1** with strong intramolecular hydrogen bonds. The other two hydroxyl groups gave a proton signal at δ 8.71.

Scheme 1. Synthesis of the BisBINOL Dialdehyde (*R,R*)-**4**

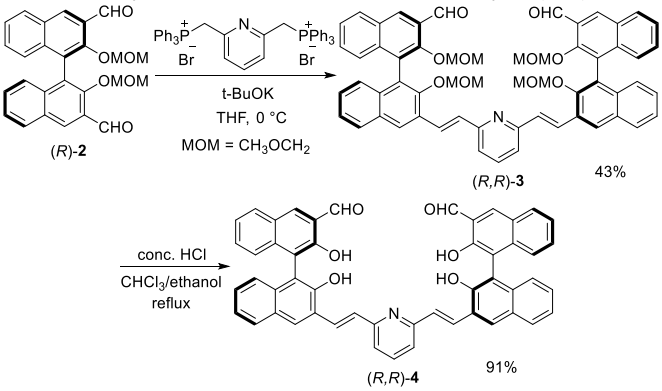

Figure 1a compares the UV-vis absorption spectra of (*R,R*)-**4** with (*R*)-**1** in methanol solution (1% DMSO). It shows that (*R,R*)-**4** has a greatly increased absorption at 355 nm which can be attributed to the π–π* transition of its more extended conjugated system provided by the divinylpyridine unit. As shown in Figure 1b, compound (*R*)-**1** is almost nonfluorescent (The signal at ~410 nm is due to the solvent-scattered light). Although the fluorescence of (*R,R*)-**4** is also very weak, it is much stronger than that of (*R*)-**1** at 455 nm (Figure 1b). That is, conversion of one of the aldehydes in a BINOL unit to the conjugated vinyl pyridine units in (*R,R*)-**4** should have reduced the excited state proton transfer-based fluorescence quenching by the intramolecularly hydrogen bonded *ortho*-hydroxyl-aldehyde units.

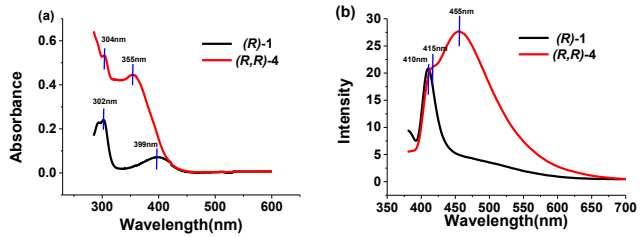

Figure 1. (a) UV-vis and (b) fluorescence spectra (λ_{exc} = 365 nm, slits: 5/5 nm) of compounds (*R*)-**1** and (*R,R*)-**4** (10 μM). (solvent: MeOH/DMSO = 99/1, v/v.)

2. Fluorescent Responses toward *L*- and *D*-Valine.

We studied the fluorescent response of (*R,R*)-**4** in combination with $Zn(OAc)_2$ toward the two enantiomers of valine. When (*R,R*)-**4** (0.01 mM in MeOH) was treated with $Zn(OAc)_2$ (5.0 equiv), almost no change in fluorescence was observed. Addition of *L*-valine (5 - 80 equiv, CBS buffer pH = 10.28) to the above (*R,R*)-**4**+$Zn(OAc)_2$ solution generated large fluorescence enhancement at λ = 550 nm (Figure 2a). However, when *D*-valine was added to the (*R,R*)-**4**+$Zn(OAc)_2$ solution, much smaller fluorescence enhancement was observed under the same conditions (Figure 2b). We studied the fluorescence response versus the reaction time. After (*R,R*)-**4**+$Zn(OAc)_2$ (5 equiv) was treated with *L*-valine (50 equiv) for 4 h, its fluorescence enhancement became stable (Figure S1). However, there was almost no fluorescence enhancement when (*R,R*)-**4**+$Zn(OAc)_2$ (5 equiv) was treated with *D*-valine (50 equiv) for over 5 h. The fluorescence responses of (*R,R*)-**4**+$Zn(OAc)_2$ with *L*- and *D*-valine (50 equiv) are compared in Figure 2c which gave an ef [enantioselective fluorescence enhancement ratio = $(I_L-I_0)/(I_D-I_0)$] of 24.2. Figure 2d plots the fluorescence intensity at 550 nm versus the valine concentration. It shows that at 50 equiv valine the enantioselectivity in the fluorescent response of (*R,R*)-**4** increased to a plateau point. We also tested the effect of the amount of $Zn(OAc)_2$ on the fluorescence response. As shown in Figure S2, the fluorescence of (*R,R*)-**4**+L-valine (50 equiv) increased greatly as the amount of $Zn(OAc)_2$ increased to 4 equiv after which there was only small change in fluorescence. When (*R,R*)-**4**+L-valine (50 equiv) was treated with $Zn(OAc)_2$, little change was observed over 1 – 20 equiv. We thus chose 5 equiv $Zn(OAc)_2$ for the subsequent fluorescence measurements.

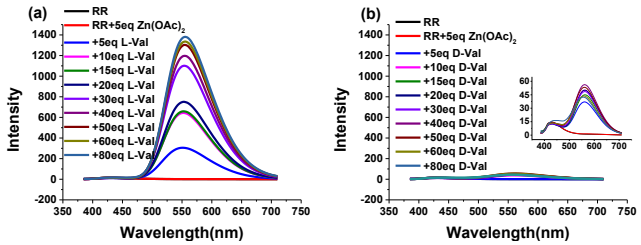

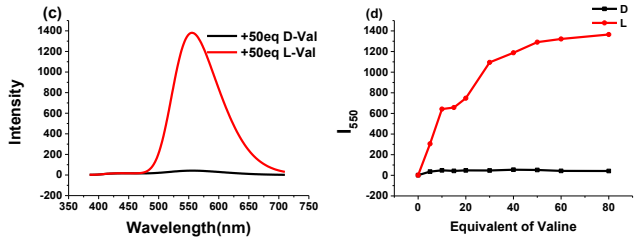

Figure 2. Fluorescence spectra of (*R,R*)-**4** (0.01 mM in MeOH, 1.0 equiv) with (a) *L*-valine (0 – 80 equiv), (b) *D*-valine (0 - 80 equiv), and (c) *L*- and *D*-valine (50 equiv) (in pH 10.28 CBS buffer) in the presence of $Zn(OAc)_2$ (5.0 equiv in MeOH) (mixed solvent: MeOH/H_2O/DMSO = 98/1/1, v/v/v). (d) Fluorescence intensity at 550 nm versus the equivalence of *L*-and *D*-valine (Reaction time, 4 h. λ_{exc}= 365 nm. Slit: 5/5 nm).

Compound (*S,S*)-**4**, the enantiomer of (*R,R*)-**4**, was prepared from (*S*)-BINOL and its interaction with *D*- and *L*-valine was studied under the same conditions as the use of (*R,R*)-**4**. Figure S3 shows that *D*-valine greatly enhanced the fluorescence of (*S,S*)-**4**+$Zn(OAc)_2$ but *L*-valine did not. Thus, the fluorescence responses of (*R,R*)-**4** and (*S,S*)-**4** toward the enantiomers of the valine display a mirror-image relationship, consistent with a chiral recognition process.

The interaction of both (*S,S*)-**4** and (*R,R*)-**4** with valine at various enantiomeric composition was studied. The fluorescence responses of these two probes versus the enantiomeric excess [ee = ([L]-[D])/([L]+[D])] of valine are given in Figure 3. These plots can be used to determine the enantiomeric composition of the amino acid.

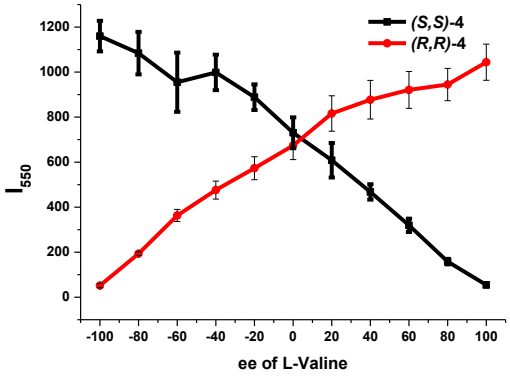

Figure 3. Fluorescence intensity of (*R,R*)- and (*S,S*)-**4** (0.01 mM in MeOH) at 550 nm in the presence of $Zn(OAc)_2$ (in MeOH, 5.0 equiv) versus the ee value of *L*-valine (in pH 10.28 CBS buffer, 50 equiv) (Error bars were obtained from three independent experiments. λ_{exc} = 365 nm. Slit: 5/5 nm).

Previously, the fluorescent response of (*R*)-**1**+$Zn(OAc)_2$ toward valine was studied but the enantioselectivity was low.[6] The greatly enhanced enantioselectivity of (*R,R*)-**4** in the fluorescent recognition of the amino acid indicates a possible cooperating effect of the two BINOL-aldehyde units in this fluorescent probe to improve the desired chiral discrimination.

3. Fluorescent Responses toward Additional Amino Acids

The fluorescent responses of (*R,R*)-**4** toward 19 common chiral amino acids (including valine) in the presence

of $Zn(OAc)_2$ were investigated. Under the same conditions, (*R,R*)-**4** showed very good enantioselective fluorescent response toward all of these natural chiral amino acids except cysteine and proline. Thus, (*R,R*)-**4** exhibits greatly expanded substrate scope over the monoBINOL probe (*R*)-**1** in the fluorescent recognition of free amino acids. Generally, the *L*-enantiomers of these amino acids caused great enhancement of the fluorescence at above 540 nm while the *D*-enantiomers didn't. Among these substrates, the ef values of (*R,R*)-**4** with 11 amino acids were observed above 10: threonine (26), valine (24), glutamic acid (23), isoleucine (17), leucine (16), phenylalanine (15), methionine (15), glutamine (14), serine (13), tryptophan (13), and histidine (10). At the same time, this probe also showed good ef values for the following 6 amino acids: asparagine (9), alanine (9), tyrosine (8), lysine (4), and aspartic acid (3) and arginine (1.5). Little fluorescence response and poor enantioselectivity were found with proline and cysteine (Figure S4). The fluorescent responses of (*R,R*)-**4** in combination with $Zn(OAc)_2$ toward 19 pairs of amino acid enantiomers are summarized in Figure 4.

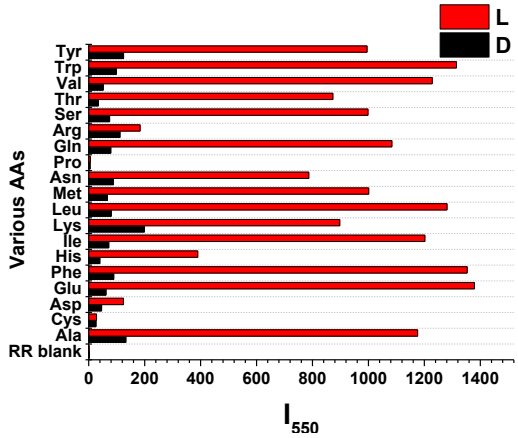

Figure 4. Fluorescent responses at 550 nm for the interaction of (*R,R*)-**4** (0.01 mM) + $Zn(OAc)_2$ (5.0 equiv) with 19 pairs of *D*-/L-amino acids (in CBS buffer, pH =10.28, 50 equiv) in MeOH. (Reaction time: 4 h. λ_{exc} = 365 nm, slits = 5/5 nm).

4. Comparison with Another bisBINOL-Based Probe

Recently, we reported another bisBINOL-based fluorescent probe (*S,S*)-**5**.[9] This compound has only two hydroxyl groups whereas (*R,R*)- or (*S,S*)-**4** has four hydroxyl groups. The structure of (*S,S*)-**5** is also more flexible without the two vinyl groups of (*S,S*)-**4** to conjugate the pyridine ring with the naphthyl rings. Thus, (*S,S*)-**5** is both electronically and sterically very different from (*S,S*)-**4**. It was found that (*S,S*)-**5** also exhibited highly enantioselective fluorescent responses toward a number of amino acids in the presence of $Zn(OAc)_2$. We have identified the following different fluorescent responses between (*S,S*)-**5** and (*S,S*)-**4**: (1) The enantioselectivity of these two fluorescent probes are the opposite even though their binaphthyl units have the same chiral configuration. For example, when (*S,S*)-**5** was treated with valine, *L*-valine greatly enhanced the fluorescence but *D*-valine did not. (2) The fluorescence enhancement and enantioselectivity of (*S,S*)-**5** in the presence of the acidic amino acids, such as aspartic acid and glutamic acid, and the basic amino acid lysine were very low. However, (*S,S*)-**4** or its enantiomer (*R,R*)-**4** showed very good enantioselective fluorescent responses toward glutamic acid (ef = 23) lysine (ef = 4), and aspartic acid (ef = 3). Thus, (*S,S*)- and (*R,R*)-**4** have also expanded the substrate scope of (*S,S*)-**5** in the fluorescent recognition of amino acids.

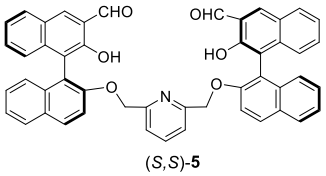

(*S,S*)-**5**

5. Study of the Interaction of $Zn(OAc)_2$ with the Imines Prepared from the Condensation of (*R,R*)-4 with *D/L*-Valine by NMR and Mass Spectroscopic Analyses

In order to gain a better understanding on the fluorescent recognition of amino acids by the new bisBINOL-based probe, we prepared the two imine compounds *L*-**6** and *D*-**6** from the condensation of (*R,R*)-**4** with *L*- and *D*-valine, respectively. The methanol solutions of these two compounds gave only very weak fluorescence. As shown in Figure 5, large fluorescence enhancement at λ = 550 nm was observed when *L*-**6** was treated with $Zn(OAc)_2$ (5.0 equiv.).). However, there was much smaller fluorescence enhancement at λ = 556 nm for the interaction of *D*-**6** with $Zn(OAc)_2$ (5.0 equiv.). Therefore, the two diastereomeric compounds *L*-**6** and *D*-**6** have produced very different fluorescent responses upon treatment with $Zn(OAc)_2$. These fluorescent responses are similar to those shown in Figure 2 for the interaction of (*R,R*)-**4**+$Zn(OAc)_2$ with the amino acid enantiomers.

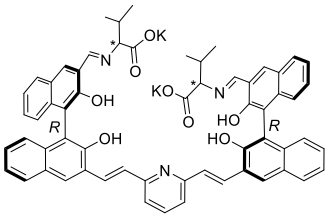

L-**6** (prepared from *L*-valine)
D-**6** (prepared from *D*-valine)

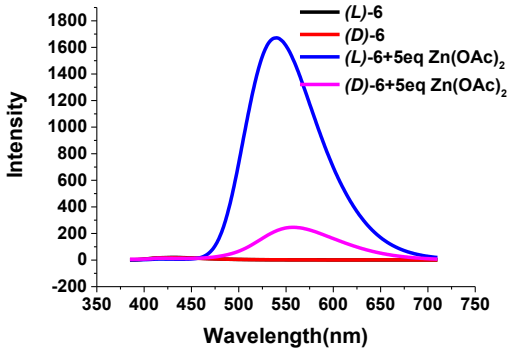

Figure 5. Fluorescence spectra of *L*- and *D*-**6** (20 μL, 1 mM in MeOH, 1.0 equiv) with $Zn(OAc)_2$ (4 mM, in MeOH, 5.0 equiv). The two components are directly added into methanol respectively which gave the final concentration of *L*- and *D*-**6** at 0.01 mM. The mixture was allowed to stand at room temperature for 1 h (λ_{exc} = 365 nm. Slit: 5/5 nm).

A ^{1}H NMR spectroscopic study was then conducted for the reactions of *L*- and *D*-**6** with various equivalents of $Zn(OAc)_2$. Upon treatment with $Zn(OAc)_2$ (0.5 - 4 equiv) in CD_3OD, though some precipitates were formed, *L*-**6** was completely converted to a new product and the ^{1}H NMR spectra gave relatively sharp signals as shown in Figure 6c,d and Figure S5-S6, indicating a well-defined structure of the product. The isolated precipitate was further dissolved in CD_3OD which gave the same ^{1}H NMR spectrum as above (Figure S7). However, under the same conditions when the diastereomer *D*-**6** was reacted with $Zn(OAc)_2$ (0.5 - 4 equiv), the ^{1}H NMR signals mostly disappeared with more precipitates produced in the NMR tube (Figure 6a,b). One hypothesis for the poor solubility of the precipitate generated from the reaction of *D*-**6** with $Zn(OAc)_2$ could be the formation of a polymeric structure from the intermolecular coordination of the imine with Zn(II) centers.

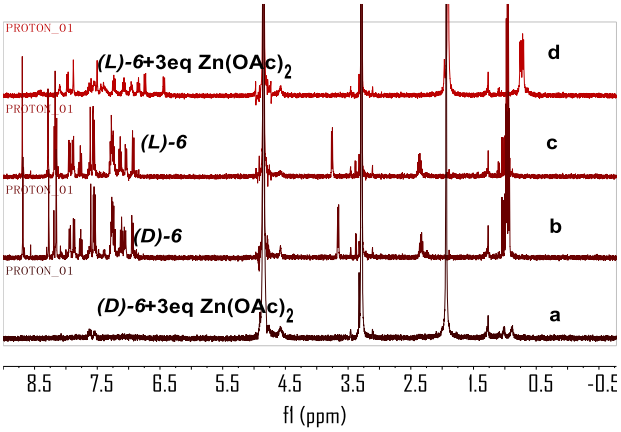

Figure 6. ^{1}H NMR spectra of *L*- and *D*-**6** titrated with $Zn(OAc)_2$ (3 equiv.) in CD_3OD for 1 h at room temperature.

The mass spectra (IT-TOF) of the reaction mixtures of *L*- and *D*-**6** with $Zn(OAc)_2$ (1 - 3 equiv) in methanol were obtained which however only gave the peaks of the imines with no information about the corresponding zinc complexes (Figure S5). This indicates that in methanol the zinc coordination may be too weak to give signals in the mass spectra.

We examined the solubility of the above two precipitates in various solvents, and found that only DMSO showed good solubility for both. In DMSO-d_6, the precipitate generated from the reaction of *D*-**6** with $Zn(OAc)_2$ was completely dissolved which gave sharp ^{1}H NMR signals as shown in Figure 7a. This suggests that the initial polymeric precipitate in methanol might have been depolymerized by coordination of DMSO with the zinc centers to form a symmetric small molecule. The product formed from the reaction of *L*-**6** with $Zn(OAc)_2$ was also completely dissolved in DMSO-d_6 which gave a ^{1}H NMR spectrum with broader signals (Figure 7d). This indicates that the structure of the *L*-**6**+$Zn(OAc)_2$ complex should be more complicated.

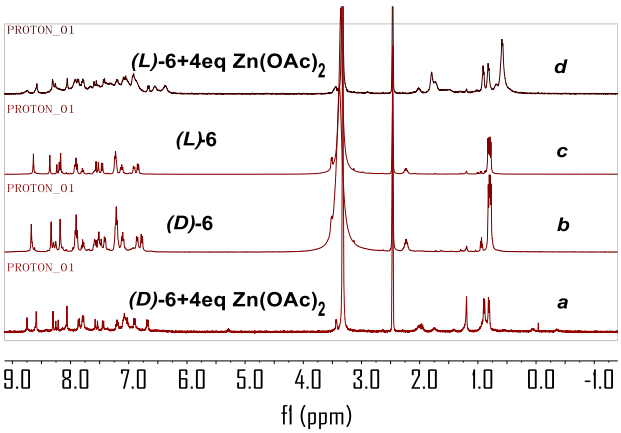

Figure 7. ^{1}H NMR spectra (in DMSO-d_6) of (b) *D*-**6**, (c) *L*-**6**, and the precipitates isolated from the reactions of (a) *D*-**6** and (d) *L*-**6** with 4 equiv $Zn(OAc)_2$ in methanol.

The above products of *L*- and *D*-**6** with $Zn(OAc)_2$ (4 equiv) in DMSO were subjected to mass spectroscopic analysis. In the mass spectrum of *D*-**6**+$Zn(OAc)_2$ in DMSO, an intense signal at m/z = 1016.2891 was observed which is consistent with the formation of a monomeric zinc complex as represented by the structure *D*-**7** (calcd for **7**+H: 1016.2889). In this structure, the zinc center may have additional coordination from the multiple nitrogen and oxygen atoms of the imine-based ligand. In the mass spectrum of *L*-**6**+$Zn(OAc)_2$, we also observed an intense signal at m/z = 1016.2899 for a similar monomeric zinc complex *L*-**7**. In addition, a significant signal at m/z (z = 2) = 1300.6426 was observed which indicates the dimerization of **7** by intermolecular coordination to multiple $Zn(OAc)_2$ units (calcd for [2x**7**+4xZnOAc+DMSO+H]/2: 2601.3538/2 = 1300.6769). Formation of this dimeric structure is consistent with the observed significantly broader signals in the ^{1}H NMR spectrum shown in Figure 7.

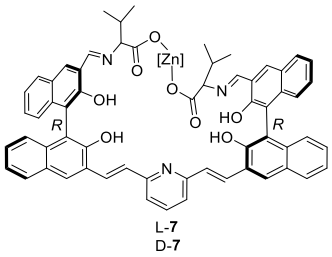

We also measured the fluorescent response of *L*- and *D*-**6** with $Zn(OAc)_2$ (5 equiv) in DMSO. They showed greatly enhanced fluorescence intensity at λ = 557 nm and 565 nm respectively but little enantioselectivity was observed (Figure S9). Thus, in DMSO, since both *L*- and *D*-**6** can react with $Zn(OAc)_2$ to form the monomeric zinc complexes like *L*- and *D*-**7** respectively which can restrict the rotation of the naphthyl rings with increased structural rigidity to give enhanced fluorescence. It is proposed that in methanol solution only the reaction of *L*-**6** with $Zn(OAc)_2$ could generate an intramolecular coordination complex like *L*-**7** to show greatly enhanced fluorescence, but *D*-**6** might prefer to undergo an intermolecular complexation with $Zn(OAc)_2$ in methanol to generate a low solubility polymeric structure that has much

lower fluorescence. Therefore, the highly enantioselective fluorescent response of the probe (*R,R*)-**4** in methanol toward the amino acids can be attributed to the different fluorescent properties of the zinc complexes of the condensation imine products formed with amino acid enantiomers.

Conclusion

We have developed a convenient synthesis of a new bisBINOL-based fluorescent probe for the recognition of amino acids. It shows very good enantioselective fluorescent responses toward 17 naturally occurring amino acids in the presence of Zn^{2+}. This substrate scope in the enantioselective fluorescent recognition of amino acids is unprecedented. Two diastereomeric imines are synthesized from the condensation of this probe with two enantiomers of an amino acid. Spectroscopic studies of the reactions of these imines with $Zn(OAc)_2$ have provided insights into the origin of the observed enantioselective fluorescent recognition of amino acids.

Experiment Section

General Information. The commercially available compounds were used without further purification unless otherwise noted. High-performance liquid chromatography or spectroscopic grade solvents were used for the optical spectroscopic studies.

Synthesis and Characterization of (*R,R*)-3. (Pyridine-2,6-diylbis(methylene))bis(triphenylphosphonium) dibromide (0.79 g, 1.0 mmol) and (*R*)-1,2'-bis(methoxymethoxy)-[1,1'-binaphthalene]-3,3'-dicarbaldehyde (*R*)-**2** (1.30 g, 3.0 mmol) were added to a dry 50 mL round-bottom flask, and then anhydrous THF (25 mL) was added. The mixture was cooled to 0 °C, and potassium tert-butoxide (0.26 g, 2.1 mmol) was added. After the reaction mixture was stirred for 3 h, it was quenched with water and extracted with ethyl acetate (2 × 15 mL). The combined organic phase was dried over Na_2SO_4. After removal of the solvent, the residue was purified by flash column chromatography on silica gel eluted with petroleum ether:ethyl acetate (10:1) to give (*R,R*)-**3** as a light yellow solid (0.40 g) in 43% yield. ^{1}H NMR (400 MHz, DMSO-d_6) δ 10.40 (s, 2H), 8.66 (s, 2H), 8.63 (s, 2H), 8.23 (m, 4H), 8.09 (d, *J* = 8.4 Hz, 2H), 7.88 (t, *J* = 7.7 Hz, 1H), 7.63 (d, *J* = 16.0 Hz, 2H), 7.58 – 7.44 (m, 8H), 7.32 (t, *J* = 8.3, 6.8, 1.3 Hz, 2H), 7.13 (d, *J* = 8.5 Hz, 2H), 7.01 (d, *J* = 8.5 Hz, 2H), 4.77 – 4.61 (m, 8H), 2.74 (s, 6H), 2.62 (s, 6H). ^{13}C{^{1}H} NMR (101 MHz, DMSO-d_6) δ 190.8, 170.4, 154.6, 153.0, 151.7, 136.2, 133.0, 132.2, 130.6, 130.2, 130.0, 129.6, 129.5, 128.7, 128.5, 127.2, 127.0, 126.4, 126.1, 125.8, 125.6, 125.4, 124.6, 121.8, 99.6, 98.8, 56.1, 55.9, 20.8, 14.1.

Synthesis and Characterization of (*R,R*)-4. Concentrated HCl (2 mL) and ethanol (1 mL) were added to (*R,R*)-**3** (205 mg, 0.22 mmol) in $CHCl_3$ (1 mL) at rt. After heated at reflux for 3 h in an oil bath, the resulting mixture was added into H_2O (10 mL) at rt which was then neutralized by using saturated $NaHCO_3$ solution until no more gas release . EtOAc (2 × 20 mL) was used for extraction and the resulting solution was concentrated under reduced pressure to give the crude product in 99% yield (181 mg, yellow solid). Further purification by column chromatography on silica gel was conducted by eluting gradiently with 25−50% ethyl acetate in hexane which afforded the product (*R,R*)-**4** as a light yellow solid in 91% yield (166 mg). ^{1}H NMR (400 MHz, DMSO-d_6) δ 10.31 (s, 2H), 10.18 (s, 2H), 8.71 (s, 2H), 8.63 (s, 2H), 8.40 (s, 2H), 8.20 (d, *J* = 16.1 Hz, 2H), 8.11 (t, 2H), 7.92 (d, *J* = 7.8 Hz, 2H), 7.80 (d, *J* = 7.7 Hz, 1H), 7.55 (d, *J* = 16.1 Hz, 2H), 7.46 (d, *J* = 7.8 Hz, 2H), 7.41 – 7.34 (m, 4H), 7.25 (t, *J* = 8.1 Hz, 2H), 7.15 (t, 2H), 6.96 (d,2H), 6.80 (d, *J* = 8.6 Hz, 2H). ^{13}C{^{1}H} NMR (101 MHz, DMSO-d_6) δ 197.3, 155.6, 154.6, 151.9, 138.1, 137.8, 137.6, 134.0, 130.7, 130.6, 129.2, 128.8, 128.6, 128.0, 127.3, 127.0, 124.7, 124.5, 124.3, 123.6, 121.7, 116.7, 114.8. HRMS (ESI) m/z: $[M + H]^+$ Calcd for $C_{51}H_{34}NO_6$ 756.2381; Found 756.2374. $[\alpha]_D^{24}$ = -36 degreem$Lg^{-1}dm^{-1}$ (c = 0.1, CH_2Cl_2).

Synthesis and Characterization of (*S,S*)-4. By using the same procedure as above, compound (*S,S*)-**4**, the enantiomer of (*R,R*)-**4**, was obtained from (*S*)-**2** in a two-step yield of 38% (yellow solid). ^{1}H NMR (400 MHz, DMSO-d_6) δ 10.35 (s, 2H), 10.21 (s, 2H), 8.75 (s, 2H), 8.66 (s, 2H), 8.44 (s, 2H), 8.24 (d, *J* = 16.1 Hz, 2H), 8.18 – 8.07 (m, 2H), 7.96 (d, *J* = 8.0 Hz, 2H), 7.84 (s, 1H), 7.59 (d, *J* = 16.1 Hz, 2H), 7.50 (d, *J* = 7.8 Hz, 2H), 7.45 – 7.35 (m, 4H), 7.29 (t, *J* = 7.0 Hz, 2H), 7.19 (t, 2H), 7.00 (d, *J* = 9.6 Hz, 2H), 6.84 (d, *J* = 8.3 Hz, 2H). ^{13}C{^{1}H} NMR (101 MHz, DMSO-d_6) δ 197.2, 155.6, 154.7, 151.9, 138.1, 137.8, 137.4, 134.0, 130.7, 130.6, 129.8, 128.8, 128.6, 127.9, 127.3, 127.0, 124.7, 124.5, 124.3, 123.68, 121.7, 116.7, 114.9. HRMS (ESI) m/z: $[M + H]^+$ Calcd for $C_{51}H_{34}NO_6$ 756.2381; Found 756.2383. $[\alpha]_D^{24}$ = +34 degreem$Lg^{-1}dm^{-1}$ (c = 0.1, CH_2Cl_2).

Preparation of Samples for Fluorescence Measurement. For each measurement, freshly prepared stock solutions of (*S,S*)-**4** and (*R,R*)-**4** in DMSO (1.0 mM), $Zn(OAc)_2$ in methanol (4.0 mM), and amino acid in pH 10.28 CBS buffer (1.0 – 20.0 mM) were used. The three components were directly added into methanol (2 mL) respectively which were then allowed to stand at room temperature for 4 h before fluorescence measurement.

Synthesis and Characterization of *L*- and *D*-6. To the stirred methanol solution of *L*-valine (23.4 mg, 0.2 mmol) deprotonated with KOH (11.2 mg, 0.2 mmol), (*R,R*)-**4** (75.5 mg, 0.1 mmol) was added. The reaction mixture was kept at rt for 5 h to yield a red solution. The completion of the reaction was monitored by using TLC. *L*-**6** was obtained as a red solid quantitatively (102.9 mg) after removal of the solvent under vacuum. ^{1}H NMR (400 MHz, CD_3OD) δ 8.70 (s, 2H), 8.29 (s, 2H), 8.22 – 8.09 (m, 4H), 7.95 (d, J = 8.2 Hz, 2H), 7.89 (d, J = 7.9 Hz, 2H), 7.77 (t, 1H), 7.62 – 7.53 (m, 4H), 7.32 – 7.21 (m, 6H), 7.13 (t, 2H), 7.04 (d, J = 7.3 Hz, 2H), 6.93 (d, J = 8.0 Hz, 2H), 3.76 (d, J = 6.0 Hz, 2H),2.40 –2.31 (m, 2H), 0.96 (dd, J = 6.9 Hz, 12H). ^{13}C{^{1}H} NMR (101 MHz, CD_3OD) δ 177.4, 165.5, 156.3, 155.9, 151.0, 137.2, 135.5, 134.1, 132.4, 131.7, 131.6, 129.3, 129.0, 128.9, 128.7, 128.6, 128.5, 128.0, 126.6, 126.5, 124.3, 124.1, 122.9, 121.5, 119.3, 115.8, 114.5, 81.1, 31.4, 19.2, 17.4. HRMS (ESI) m/z: $[M-2K+3H]^+$ Calcd for $C_{61}H_{52}N_3O_8$ 954.3749; Found 954.3708.

By using the same procedure as described above, compound *D*-**6** was obtained from the reaction of (*R,R*)-**4** and *D*-valine in 100% yield as a red solid. ^{1}H NMR (400 MHz, CD_3OD) δ 8.68 (s, 2H), 8.27 (s, 2H), 8.20 – 8.12 (m, 4H), 7.94 (d, *J* = 8.4 Hz, 2H), 7.87 (d, *J* = 8.0 Hz, 2H), 7.75 (t, *J* = 7.9 Hz, 1H), 7.60 – 7.50 (m, 4H), 7.33 – 7.18 (m, 6H), 7.11 (t, 2H), 7.06 (d, *J* = 8.4 Hz, 2H), 6.94 (d, *J* = 8.3 Hz, 2H), 3.66 (d, *J* = 6.4 Hz, 2H), 2.38 –2.29 (m, 2H), 0.96 (dd, *J* = 16.0, 6.8 Hz, 12H). $^{13}C\{^1H\}$ NMR (101 MHz, CD_3OD) δ 177.1, 165.4, 156.2, 155.8, 150.8, 137.2, 135.4, 134.0, 132.3, 131.7, 131.6, 129.3, 128.9, 128.8, 128.7, 128.6, 128.5, 127.9, 126.5, 125.8, 124.4, 124.0, 122.9, 121.5, 119.5, 115.8, 114.4, 81.6, 31.4, 19.0, 17.6. HRMS (ESI) m/z: $[M-2K+3H]^+$ Calcd for $C_{61}H_{52}N_3O_8$ 954.3749; Found 954.3631.

Isolation of the Products for NMR Measurements in Figure 7. $Zn(OAc)_2$ (4.0 equiv, 1.0 mL, 4.0 mM in MeOH) was added to a solution of *L*- or *D*-**6** (1.0 mL, 1.0 mM in MeOH) which reacted quickly to produce turbid solution containing precipitates. The precipitates were isolated after centrifugation which were then washed with methanol for three times (3 × 2 mL) and dried before they were dissolved in DMSO-d_6 for NMR analyses.

Supplementary Information Available: Additional spectroscopic data are included.

Key words: Fluorescent sensing, amino acids, BINOL, enantioselective, zinc(II)

Acknowledgement: This work was financially supported by Sichuan Science and Technology Program 2021YJ0398. LP thanks partial support of this project by the US National Science Foundation (CHE-1855443).

References

1. Pu, L. Enantioselective Fluorescent Recognition of Free Amino Acids: Challenges and Opportunities. *Angew. Chem. Int. Ed*. **2020**, *59*, 21814-21828.
2. Y. Zhou, J. Yoon, Recent Progress in Fluorescent and Colorimetric Chemosensors for Detection of Amino Acids. *Chem. Soc. Rev*. **2012**, 41, 52–67.
3. J. Wang, H. Liu, Z. Tong, C. Ha, Fluorescent/Luminescent Detection of Natural Amino Acids by Organometallic Systems. *Coord. Chem. Rev*. **2015**, 303, 139-184.
4. Reviews on enantioselective fluorescent recognition: (a) L. Pu, Fluorescence of Organic Molecules in Chiral Recognition. *Chem. Rev*. **2004**, 104, 1687–1716. (b) D. Leung, S. O. Kang, E. V. Anslyn, Rapid Determination of Enantiomeric Excess: A Focus on Optical Approaches. *Chem. Soc. Rev.* **2012**, 41, 448–479. (c) A. Accetta, R. Corradini, R. Marchelli, Enantioselective Sensing by Luminescence. *Top. Curr. Chem.* **2010**, 300, 175–216. (d) X. Zhang, J. Yin, J. Yoon, Recent Advances in Development of Chiral Fluorescent and Colorimetric Sensors. *Chem. Rev.* **2014**, 114, 4918-4959. (e) B. T. Herrera, S. L. Pilicer, E. V. Anslyn, L. A. Joyce, C. Wolf. Optical Analysis of Reaction Yield and Enantiomeric Excess: A New Paradigm Ready for Prime Time. *J. Am. Chem. Soc.* **2018**, 140, 10385-10401.
5. Selected references on enantioselective fluorescent recognition of amino acids: (a) S. Pagliari, R. Corradini, G. Galaverna, S. Sforza, A. Dossena, M. Montalti, L. Prodi, N. Zaccheroni, R. Marchelli, Enantioselective Fluorescence Sensing of Amino Acids by Modified Cyclodextrins: Role of the Cavity and Sensing Mechanism. *Chem. Eur. J*. **2004**, 10, 2749–2758. (b) L. Yang, S. Qin, X. Su, F. Yang, J. You, C. Hu, R. Xie, J. Lan, 1,1'-Binaphthyl-based Imidazolium Chemosensors for Highly Selective Recognition of Tryptophan in Aqueous Solutions. *Org. Biomol. Chem*. **2010**, 8, 339–348. (c) R. Freeman, T. Finder, L. Bahshi, I. Willner, β-Cyclodextrin-Modified CdSe/ZnS Quantum Dots for Sensing and Chiroselective Analysis. *Nano Lett.* **2009**, 9, 2073-2076. (d) W. Wei, K. Qu, J. Ren, X. Qu, Chiral Detection Using Reusable Fluorescent Amylose-Functionalized Graphene. *Chem. Sci*. **2011**, 2, 2050-2056. (e) L. Song, S. Wang, N. A. Kotov, Y. Xia, Nonexclusive Fluorescent Sensing for L/D Enantiomers Enabled by Dynamic Nanoparticle-Nanorod Assemblies. *Anal. Chem*. **2012**, 84, 7330−7335. (f) F. Song, N. Fei, F. Li, S. Zhang, Y. Cheng, C. Zhu, A Chiral Ionic Polymer for Direct Visual Enantioselective Recognition of α-Amino Acid Anions. *Chem. Commun.* **2013**, 49, 2891-2893. (g) Wu T, Kessler J, Bouř P. Chiral sensing of amino acids and proteins chelating with EuIII complexes by Raman optical activity spectroscopy. J. Phys. Chem. Chem. Phys. **2016**, *18*, 23803-23811.
6. Z. Huang, S. Yu, K. Wen, Y. Yu, L. Pu, Zn(II) Promoted Dramatic Enhancement in the Enantioselective Fluorescent Recognition of Functional Chiral Amines by a Chiral Aldehyde. *Chem. Sci*. **2014**, 5, 3457–3462.
7. (a) H. Brunner, J. Goldbrunner. Asymmetrische Katalysen, IL: Optisch aktive Binaphthylderivate—Synthese und Einsatz in Übergangsmetallkatalysatoren. *Chem. Ber.* **1989**, *122*, 2005–2009. (b) H. C. Zhang, W. S. Huang, L. Pu. Biaryl-based macrocyclic and polymeric chiral (salophen) Ni (II) complexes: synthesis and spectroscopic study. *J. Org. Chem.* **2001**, *66*, 481–487.
8. K. Fuji, K. Ichikawa, and E. Fujita. Lythraceous Alkaloids. Part 11. Total Synthesis of (±)-Lythranidine. *J. Chem. Soc. Perkin Trans 1* **1980**, 1066-1069.
9. Zhu, Y.-Y.; Wu, X.-D.; Gu, S.-X.; Pu, L. Free Amino Acid Recognition: A Bisbinaphthyl-Based Fluorescent Probe with High Enantioselectivity. *J. Am. Chem. Soc*. **2019**, *141*, 175−181.

Graph for Table of Content

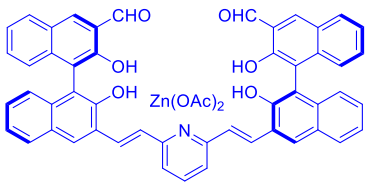

Highly enantioselective fluorescent probe for a broad range of amino acids